D16

N78-32482

APPLICATION OF NASTRAN TO TFTR TOROIDAL FIELD COIL STRUCTURES*

S.J. Chen
EBASCO Services, Incorporated

E. Lee
Grumman Aerospace Corporation

SUMMARY

The application of NASTRAN to the structural analysis of the Tokamak Fusion Test Reactor (TFTR) Toroidal Field (TF) magnetic coils and their supporting structures are described in this paper. The primary applied loads on the TF coils are electromagnetic and thermal. The complex structure and the tremendous applied loads necessitated computer type of solutions for the design problems. In the early stage of the TF coil design, many simplified finite element models were developed for the purpose of investigating the effects of material properties, supporting schemes, and coil case material on the stress levels in the case and in the copper coil. In the more sophisticated models that followed the parametric and scoping studies, the isoparametric elements, such as QUAD4, HEX8 and HEXA, were used. The analysis results from using these finite element models and the NASTRAN System were considered accurate enough to provide timely design information. These analytical results were further confirmed by using the EBASCO developed isoparametric composite element.

INTRODUCTION

The TFTR, now under construction and expected to be operational by 1981, will be the first Tokamak in the world to produce 14 MeV fusion neutrons and 3.5 MeV fusion alpha particles in a break-even experiment involving a deuterium-tritium plasma. The information to be obtained from the TFTR project will contribute to the effort aimed at the construction of demonstration fusion power reactors in the early 1990s. This would help meet our nation's energy demands.

The main components of the TFTR are the large doughnut-shaped vacuum vessel (or torus) which contains the plasma and the TF coils which generate the magnetic field for plasma confinement (see Figure 1). There are 20 TF coils (see Figure 2); each coil has 44 turns of copper winding which are insulated from one another. The coils are wrapped in epoxy and placed in a structural

---

*The work described herein was performed pursuant to Princeton Plasma Physics Laboratory's Subcontract No. 258, under ERDA Contract No. EY76-C-02-3093 with Princeton University.

246

case (see Figure 3). These coils are supported near the machine's center (see Figure 1) by an inner ring and column system and outboard of the coils by outer shear-compression members (see Figure 4).

The coils are operated in a pulsed mode with the current increased from zero until the desired magnetic field strength is reached. The field is held constant (flat top) for approximately 3 seconds before decreasing. The minimum time between pulses is 300 seconds; the coils are required to sustain 300,000 full-power pulses. Heat generated by the electric current in the copper coils is removed by cooling water flowing through the coils at an inlet temperature of 10°C (50°F) and an outlet temperature not more than 68.3°C (155°F).

The primary applied loads on the TF coils are electromagnetic and thermal. There are two electromagnetic loads; one is due to the interaction of the toroidal current and its field which results in a net centering force of 27 076 kN (6087 kips). The other electromagnetic load is due to the interaction of the toroidal current and the Equilibrium Field (EF) which results in a lateral moment of 11 890.0 kNm (105 240 inch-kips) (see Figure 5). The thermally-induced load is mainly due to temperature difference between the copper winding and the coil case.

The complex structure and large applied loads necessitated computer-based analysis for solutions to various design problems. In order to investigate the effects of material properties, supporting schemes, coil case material and manufacturing tolerances on the stress levels in the case and in the coil, simplified finite element models were developed and analyzed using NASTRAN. In the more sophisticated models that followed the parametric and scoping studies, isoparametric elements such as QUAD4, HEX8 and HEXA were used.

This paper will describe the various finite element models that were used in support of the coil design. In addition, the element types, size of each model, multi-point constraints and cyclic symmetry features of NASTRAN are discussed. The analytical results and correlations among the various models are also presented. A comparison of the results obtained using the common NASTRAN isoparametric elements with results obtained using the EBASCO-developed composite isoparametric element will be included.

FINITE ELEMENT MODELS

The finite element method was employed in the structural analysis of the TF coils. Several models of the TF coil were generated during the preliminary and the detailed design phases of the Tokamak Project. They can be categorized as follows:

- Simplified 2-D and 3-D Models
- Detailed 3-D Model
- Detailed Local Models
- Detailed 3-D EBASCO developed Composite Element Model.

The first group of finite element models (FEM) was used primarily during the preliminary design phase, where numerous studies were conducted to achieve an optimum TF coil design with respect to coil shape and coil support schemes. Since the preliminary design phase is characterized by fast design changes, the FEMs must be simple enough for modifications to be accomplished in a short time and the results generated must meet the design objectives. The first three FEMs, summarized in Table I, are considered as Simplified 2-D and 3-D models. TF1G3D was later modified to include dynamic, fault and seismic analyses.

Following the completion of the design studies using the Simplified Models, a preliminary design configuration of the TF coil assembly was subjected to a more detailed stress analysis. The second generation 3-D model (TF2G3D in Table I) was developed for this effort. This model includes the TF coil, outboard inter-coil shear compression box and the inner rings attached to the central column. Analytical results from this model had shown that the stresses in the epoxy and the copper winding in the vicinity of the ring supports were high, but this model was not fine enough to provide accurate results required. Since the demand for design information in the epoxy, copper, coil case bolts and the bolts in the yoke were of such a detailed nature, Detailed Local Models were developed. These models are summarized in Table I as TF3G2D, TF3G3D, 90° Yoke Segment, and Local Stress Concentration.

These models provided timely information for the TF coil design effort from the preliminary design to a final design phase of the Tokamak Program. In the meantime, a more sophisticated isoparametric composite element was being developed. A model using the composite element was generated to confirm the results produced by previous models using available NASTRAN elements, as well as to verify the structural integrity of the TF coil.

A more detailed description of the above mentioned FEMs are presented in the following paragraphs.

First Generation 2-D Model (TF1G2D)

The purpose of this model was to study the different coil shapes and to investigate various support conditions.

The first generation 2-D model consisted of three different models: the circular shape, the dee shape and the tear drop shape, which was basically the dee shape turned around. Due to the symmetric condition of the geometry, as well as the loading (TF force), only one-half the coil was considered in this model, along with its supports.

The coil was represented by a one-line model consisting of beam elements, with the nose and outboard supports simulated by spring elements (see Figure 6). All of the beam elements had six degrees of freedom per element, while the springs had two degrees of freedom per element.

For all analyses, both homogeneous and composite section properties were considered, along with the change of the cross section due to the wedge at the

nose. These properties were calculated at the center of each member, while also applying a factor of the ratios of the Young's moduli of the steel and copper, in order to compensate for the different materials.

The model had support points along the horizontal line of symmetry. These points were assumed to only have the freedom of horizontal displacement. The supports at the outboard inter-coil connections were simulated as horizontal springs whose stiffnesses were calculated based upon the resistance capability of the connections in the horizontal direction. At the nose, the coil originally had a wedge support where the side plates of the steel casing actually came in contact with the adjacent coils, providing resistance to horizontal displacement. In later design, this was replaced by support rings coming from a center column. All three models were considered with the wedge support, and in addition, the circular shape model was analyzed with the support rings. The values of these spring constants depended on the stiffness of such support.

Second Generation 2-D Model (TF2G2D)

The purpose of this model was to understand the force and moment transmitted from the copper winding, through the epoxy, to the steel case, as the coil was subjected to the toroidal field force. This study included the effects of shear modulus in epoxy, the Young's modulus of the copper winding, and the failure of the epoxy in shear.

Due to the symmetric condition of the geometry, as well as the loading (TF force), one-half of the coil with the supports was considered in this model.

The model consisted of three radii, with the inner and outer ones containing the steel casing grid points and the middle one for the copper grid points. When the constant copper cross-section design was introduced, another radius, coincident with the copper grid point radius, was added for additional steel casing grid points. This was needed in order to create a finer mesh to handle the varying thickness of the side plates.

In the model, the steel casing, including outer and inner flanges, and the side plates were modeled as BAR (beam) and QDMEM2 (quadrilateral membrane) elements, respectively. The copper winding was modeled as BAR elements which connected the copper nodal points located in the middle of the coil. The epoxy between steel casing and the copper winding were represented by ROD (beam with pin connections) and SHEAR elements. The cross-sectional areas of ROD and SHEAR elements were calculated based on the equivalent stiffness of the epoxy in resisting the relative movement of the steel casing and the copper winding in radial and tangential directions, respectively. The supports at the nose and the outboard box of the coil basically resisted the movement of the steel casing in the horizontal direction and were modeled as horizontal springs (ELAS2).

Many cases have been investigated with this model and various support schemes have been analyzed. The bond in the epoxy between the copper bundle and the casing have been considered, as well as the case of no bond in epoxy.

Analysis has also been performed to determine the redistribution of stresses, moments, and forces with varying material and cross-sectional properties. This model has also been used to determine the effect of having a gap between the coil and support rings. In addition, various analyses have been performed using the constant copper cross-section design.

The results obtained from these analyses included displacements of grid points, loads in the copper, forces at the supports, and the forces and stresses in the steel casing, copper, and epoxy. All of these results were obtained for both toroidal field (TF) loads and for thermal loads.

First Generation 3-D Model (TF1G3D)

This model, shown in Figure 7, was originally generated to investigate support schemes for the TF coil subjected to out-of-plane loading. It was later modified for dynamic (EF out-of-plane), faulted (TF coil short circuits) and seismic analyses. This coarse type model was selected to avoid the expensive computer cost usually incurred in analyses for dynamic and nonsymmetric static loads. It was estimated that the effects of these loads are minor on the stress in the critical region of the TF coils and the inner support structure (ISS) compared with the normal operating electromagnetic static loads. This model can give a qualitative comparison of TF coil and ISS stress results, and reasonably accurate results for reaction forces at the support pedestals and floor system. This section first describes the finite element model used in the nonlinear dynamic analysis performed for the out-of-plane TF coil pulse loading induced by the interaction of the EF coil magnetic field with the TF coil electrical current field, and then describes the modifications made to this model in the seismic and faulted load analyses.

Dynamic Analysis Model - This model has taken into account the geometric nonlinearity associated with the TF coil pedestal supports, which prevent horizontal lateral displacement of the TF coil in only one direction. Structural damping was also included.

Because of the geometric rotational symmetry of the TF coils, ISS and floor system, a three-dimensional finite element model of a 36° segment of the structure, composed of one-dimensional and two-dimensional finite elements, was used in the analysis (see Figure 7). The model was sufficiently detailed so that the effects of the TF coil pulse loading, seismic loads and fault loads could be determined, but local structural details, such as keyed and bolted splices and cutouts, were not incorporated into the model. A total of 262 nodal points and 248 finite elements (114QUAD4, 76BAR, 44RBAR, 12ROD, 2CELAS2) were used.

The TF coils, represented by BAR elements, were connected to the support pedestals by means of RBAR elements and CELAS2 spring elements which take into account the coil base pedestal stiffness. These connections provide horizontal lateral load transfer from the TF coils to the pedestals. At these connection points between coil base and pedestal top, a nonlinear transient force-displacement relationship was defined to represent the nonlinear behavior of the pedestal support system. This geometric nonlinearity is such that

the restraint imposed on the coil base is a function of the direction of the relative horizontal lateral displacement between the coil base and the pedestal. Physically, this restraint is provided by a snubber plate against which one side of the coil base initially rests. The snubber plate location alternates from side to side, from coil to coil. Under load, when the coil base tends to displace such that it bears against the snubber, resistance to that displacement is provided. When the coil base displaces away from the snubber, it can do so freely and without restraint.

The floor structure was modelled as a system of QUAD4 elements and BAR elements. Connection of the pedestals to the midheight of the floor were made with REAR elements.

The TFTR structure is externally supported at the machine floor level by connection of the outer edge of the machine floor to vertical columns and the building floor system, and by connection of the inner edge of the floor system to vertical columns. These external boundary conditions were incorporated into the finite element model by fully restraining all degrees of freedom at the outer edge of the machine floor (3 displacements and 3 rotations). The vertical floor columns were not incorporated into the model because their effect on the analyses performed is negligible.

To simulate the symmetric behavior of the structure, boundary condition relationships equating displacements and rotations at boundary grid points were imposed.

Model Modifications for Seismic and Faulted Load Analyses - The primary modifications made to the model for the seismic and faulted load analyses were related to the boundary conditions. Since these loads were not rotationally symmetric like the dynamic load, the symmetric boundary condition used in the dynamic analysis was not valid. NASTRAN's cyclic symmetry features were used to represent the entire 360° structure, including 20 TF coils. In order to use the cyclic symmetric features, the non-linear connections between the TF coils and the tops of the pedestals were removed. It was assumed that only one out of every pair of coils was connected to the support pedestal. The floor system, which has a minor effect on these analyses, was totally restrained to reduce the problem size.

Second Generation 3-D Model (TF2G3D)

The first generation finite element models described in previous paragraphs were used mainly in the preliminary design of the TF coil, in the selection of coil shapes, and finally in the baseline design. Having designed a baseline TF coil, the next step was to perform more detailed stress analyses. In order to support the detailed design phase of the TF coil, a more sophisticated finite element model was required. The second generation 3-D model was developed for this effort. This model is a three-dimensional finite element model which includes the TF coil, outboard inter-coil support box and the inner rings attached to the central column support. The second generation 3-D finite element model represents an 18° sector which includes part of the ring and column support, one coil, and two half shear-compression supports from

each side of the coil (see Figure 8). The coil case is simulated by plate elements (QUAD2, TRIA2) with inplane and bending stiffnesses.

There are 44 copper windings in each coil; they are electrically isolated from each other and the coil case. The copper windings are represented by four solid elements (HEX8), and they are separated from the coil case by the epoxy and the electrical insulating material.

The center column and ring supports and the outboard inter-coil shear-compression boxes are represented by plate elements. The TF coil finite element model is supported at the bottom of the coil. This pedestal support allows the coil to move in the upward direction (no hold-down) but supports the weight and loads in the downward direction. In addition, the coil is allowed to move laterally (perpendicular to the coil plane), but is restrained by a key in the opposite direction. Radially from the device center, the coil is unrestrained. The coil nose area is connected in three directions to a 4-ring system. The two outer rings are in turn attached to the central cylinder only in the tangential direction, normal to the coil plane. The inner rings, however, are rigidly connected to the central cylinders.

The cyclic symmetry capability of NASTRAN was used to effect the remaining 19 sections of the TF coil system. The boundary points are defined as input to the program. The computer time was excessive when cyclic symmetry was used. Since the structural analysis of the baseline configuration was mainly using symmetric load, the multipoint constraints (MPC) can be used on the boundary points and, therefore, one coil model is needed. The computer time has been reduced considerably by using the MPCs. However, for unsymmetric loading, the cyclic symmetry must be used.

The epoxy bond between the copper and the coil case may have been separated during the curing process. In order to simulate this condition in the finite element model, the epoxy can have only compressive strength. When the result showed any epoxy spring element that was in tension, the spring element was eliminated from the model. After several iterations, all spring elements that were in tension were eliminated from the model. The results were representative of the no epoxy bond case.

The second generation 3-D TF coil finite element model has 1006 grid points, 1274 elements (46 TRIA2, 524 QUAD2, 176 HEX8, 528 ELAS2), and 4239 degrees of freedom. A typical run of this model, employing MPC boundary conditions, had used approximately 3000 system resource units (SRU) of computer time, whereas a run using cyclic symmetry had used three times as much time.

There were several NASTRAN runs made using the 3-D model in direct support of the TF coil design effort. The effect of different materials (e.g., titanium or steel) for the coil case and the inner support structure was investigated. Studies were done to vary the location and number of rings for the central column support. Varying thicknesses of the coil outer flange was also analyzed using the 3-D model.

The grid point forces and displacements, element forces, and stresses are printed output from the NASTRAN run. Some of the results are usually summa-

rized manually to provide immediate design information. However, the amount of data remaining to be summarized was massive; therefore, it was imperative that a computer aided post-processing program be developed. The output of these FORTRAN programs was in both tabulated and plotted formats. Plots of shear load per unit length for the inner and outer flanges were made. These plots provided the designer with the necessary information for sizing the bolts required for fastening the coil sideplate to the inner and outer flanges. These plots and tabulated data were subsequently used for fatigue analysis. In addition to these plots, copper hoop stress, epoxy normal stress, and casing membrane stress intensity were also plotted.

The copper stresses were printed in the basic rectangular coordinate system; however, this was not convenient for evaluation. The latest version of NASTRAN with the HEXA element has rectified this shortcoming. However, the corner stress "jump" for the solid element was very disturbing. Fortunately, the copper hoop stress was reasonably accurate when the 4-corner HEXA stresses were arithmetically averaged. This was perhaps due to the fact that there was no applied load in that direction. In the radial direction, the HEXA stresses cannot be simply "averaged". It was estimated using the grid point force output. More experience is required for the interpretation of the solid element stress output.

Third Generation 2-D Model (TF3G2D)

Since the inter-laminar epoxy stresses from the second generation 3-D model were obtained from a relatively crude epoxy/copper simulation, a more detailed third generation 2-D model (TF3G2D in Table I) was developed. Symmetry required only half of the coil in the model (see Figure 9). Bar elements were used for copper layers and inner and outer flanges of the case. A shear panel provided only shearing strength for the copper-to-copper and copper-to-case interfaces. A rod element provided two degrees of freedom which gave direct relative motion of the interfaces. An energy equivalence was made to obtain a spring constant for the rod and a shear strength for the shear panel. In addition to the elements in the bar-shear-spring model, a membrane element was applied in TF3G2D. This type of element was used to simulate the in-plane deformation and strength of the case side plates.

Local bending and tangential extension of all grid points at both ends of the half coil were restrained due to symmetry. Rod elements provided horizontal elastic supports at center column ring supports and connecting box supports. An energy equivalent was made for those rod elements to obtain the proper stiffness constants.

The number of nodal points for a representative model of this kind was 612, which resulted in 1604 degrees of freedom. The two-dimensional elements included 900 bars, 480 rods, 120 membranes, and 390 shear panels. Total number of force units applied to the system, for magnetic force in static analysis alone, was 434. Number of variable temperature grids was 588. Average computing time for each run was 648 system seconds on a CDC-6600 for three loading cases.

Third Generation 3-D Local Model (TF3G3D)

The third generation 2-D model described in the previous paragraphs was used to investigate shear stress distribution in epoxy due to in-plane loads (TF and thermal). The third generation 3-D local model (see Figure 10) was used primarily for the study of the shear stress in the epoxy and copper stress due to in-plane and out-of-plane (EF) loads at the critical area.

To keep the model small enough to be analyzed in the current computer and still render good critical stress data, a portion of the TF coil was analyzed. This local model consisted of the coil cut from horizontal zero degree plane and approximately 54-degree plane from the horizontal. By applying a symmetric and an anti-symmetric boundary condition to the model, a cut was made to the middle plane which was the separation of the reverse copper winding by a barrier strip. The barrier strip retained full capability of bonding; however, the bonding between the copper bundle and the case was removed except where the compression was developed by the combined loads. The nose supporting ring was simulated by springs in all directions. Boundary forces were applied to the 54-degree cross section. These forces were obtained through global 3-D model. Magnetic loads and thermal data were carefully distributed to all grid points of the model. It was the thinner copper layer and the flexibility of the layer in the other direction that made the usage of plate elements in 3-D model. TF load applied to the model included a radial in-plane load and a transverse out-of-plane load which squeezed the copper to the barrier strip.

The differences between this model and the third generation 2-D model were that plate elements were used in the 3-D model to represent copper layers, whereas bar elements were used in the 2-D model. In addition, solid elements were used in the 3-D model for the outer flange, whereas bar elements were used in the 2-D model. Due to the geometric complexity and the thickness variation of the outer flange, the solid element was used. Two types of solid elements were used in the 3-D model. A HEXA element had eight nodal points at the corners. Each corner had three translational degrees of freedom. Two HEXA elements used in the model had extra points along the edges for the proper modeling of wedge transition. A WEDGE element had six nodal points at the corners. Each corner had three translational degrees of freedom. HEXA elements were used also for the barrier strip. Plate elements used for copper, side wall, and inner flange were QUAD4s. A QUAD4 element had four nodal points at the corners and each nodal point had five degrees of freedom. The cooling hole stiffness was reduced by using offset capability of QUAD4. Shear panels used in the model were SHEAR's which were obtained from energy equivalent. The shear panels had only shear capability and each panel had four degrees of freedom. These panels connected the copper layers in two ways. A series of shear panels took the resistance of slip between copper layers in tangential direction and the other series of shear panels prevented copper from relative movement in the transverse out-of-plane direction. Finally, a set of two degrees of freedom rod elements provided compressibility of copper layers and epoxy which wrapped copper layers and copper bundle. The connection between the outer flange and the side wall was accomplished with bars and rods.

The number of grid points in the system was 2,347. It had 10,761 degrees of freedom for symmetric load condition and 11,231 degrees of freedom for anti-symmetric load condition. The number of total bulk data lines (or cards) was 14,894. Total execution time in SRU was 14,610 on a CDC-6600 for three subcases and two subcombs by NASTRAN code.

TF Coil Yoke Finite Element Model

The yoke finite element model is a 90° segment (90° - 180°) taken from the second generation 3-D model. The boundary loads were based on the TF2G3D model. The main objective of the 90° segment yoke model was to ascertain the bolt loads between the yoke and the coil case, and between the yoke and the shear-compression box (see Figure 11). Revisions to the yoke model required fewer manhours and computer usage time compared to the full coil model. Therefore, this model was used for yoke design support and parametric studies. The yoke model includes all elements associated with the second quadrant (90° - 180°) of the second generation 3-D TF coil model. The coil case is simulated by plate elements (QUAD4, TRIA3) with inplane and bending stiffnesses. The copper windings are represented by 6 solid elements (HEXA); they are separated from the coil case by the epoxy and the electrical insulating material. Due to design considerations, the epoxy material between the copper winding and the casing is assumed to take compression loads only, and has no shear or tension capabilities. The spring element (ELAS2), which has two degrees of freedom, is used to simulate these compression forces.

The bolt shear and contact stiffnesses are simulated by using the spring element (ELAS2). The yoke and shear-compression box are simulated by plate elements. A typical section is shown in Figure 11. The bolt shear stiffnesses were calculated by assuming that the parent material had yielded to 2% of the bolt diameter, and these stiffnesses were beamed to the nearest grid points.

The coil case is made of steel; the gages at the side wall, outer and inner flanges are 2.9 cm (1 1/8 in.), 14.6 cm (5 3/4 in.), 6.9 cm (2 3/4 in.), respectively. The shear-compression box and yoke assembly are shown in Figure 11.

The yoke model uses the NASTRAN multipoint constraints (MPC) at the shear-compression box boundary points. The boundary loads at both 90° and 180° are calculated using the TF2G3D model.

The contact stiffness between the shear-compression box and the yoke and the bolt axial stiffness are simulated by using spring elements. When the contact spring elements are in tension, they are eliminated from the input data set. When the bolt is in tension, the tensile stiffness is used.

The yoke finite element model has 616 grid points, 922 elements and 3,696 degrees of freedom. The computer time usage is 1,500 seconds (SRU).

Local Stress Concentration Model

The fatigue life requirement is one of the critical items in the TF coil design. A better understanding of the peak stress (including stress concentration) distribution around the bolt hole of the coil casing is essential to the estimation of the fatigue life. The primary contributors to the peak stress around the bolt hole are the bypassing stress (hoop tension) and the pin loads (both tangential and radial directions). Because of the complicated nature of the casing geometry, the effects of the by-passing stress and the pin loads are coupled. It implies that without knowing the load path around the bolt hole, it is difficult to predict how much of the peak stress is contributed by the by-passing stress or by the pin loads. Therefore, a finite element analysis was initiated to study the load path in the critical bolt hole and predict the critical peak stress. The finite element model included a segment of side plate with the critical bolt holes connecting the inner flange.

The "Multilevel Superelements" approach available in the NASTRAN program was chosen in this analysis. The advantage of the superelement approach is to allow a fine mesh model near the critical bolt holes, but a coarse mesh away from the critical area without losing the accuracy. Moreover, it is only required to have one fine mesh bolt hole model which can be repeated as many times as desired to simulate a series of bolt holes.

Two mesh generators were written to automatically generate two separate models. One is the coarse mesh model, designated as the residual superelement (see Figure 12), which included a segment of the side plate, including the bolt holes away from the critical area. The other is the fine mesh model of a typical bolt hole, designated as the primary superelement (see Figure 13). Then any number of the secondary superelement, which is similar to the primary superelement, can be automatically generated. Figure 14 shows the combined geometry of the residual and primary superelements, and indicates the location of two secondary superelements. The mesh generators were programed to include the parameters, such as diameter of bolt hole, pitch of bolt hole, numbers of bolt holes and the dimensions of the side plate segment.

The model is two-dimensional. The quadrilateral (QUAD4) and triangular (TRMEN) plate elements were used in the residual superelement, while the TRMEN element was used in the primary superelement. The QUAD4 element has eight degrees of freedom, while TRMEN has six degrees of freedom.

The force boundary condition was used to describe the boundary at the edges of the side plate segment and the pin loads acting on the bolt hole. These data were obtained from the result of 3-D analysis (TF2G3D model). The residual superelement model was used to check these applied forces for the static equilibrium. The stresses in the side plate resulting from the equilibrium check run were also compared with the 3-D result. The uniform radial pressure distribution was assumed for the pin loads acting at the primary and secondary superelements.

Three different loading conditions were considered for each model: pin loads in both tangential and radial conditions, pin load in tangential direc-

tion only (shear key to take radial shear), and no pin load. The "no pin load" condition was not the real design option being considered. However, it was included to approximately simulate the condition if the friction took all the shear loads. For all loading cases, the stress printouts plus the stress contour plots for the maximum principal stress were obtained directly from NASTRAN runs.

Composite Element 3-D Model

This model uses the EBASCO developed 3-D solid composite elements for heterogeneous material. These elements simulate the composite action of the copper and epoxy bundle and also give detail stress information in both copper and epoxy. The composite element is defined by 8 to 20 nodes.

The coil case was represented by composite elements with homogeneous isotropic properties. There were two radial layers to represent the 5 3/4 inch thick outer flange. The yoke, inter-coil shear compression boxes, pedestal support, and support rings at the nose were also modeled using the composite element. The composite element TF coil model has 2567 grid points, 740 composite elements, and 736 non-linear spring elements. Further discussion and theoretical presentation of the composite element can be obtained from references 1 and 2, respectively.

DISCUSSION OF MODEL RESULTS

Representative results from the previously described finite element models are discussed in the following paragraphs.

Figure 6 shows the various coil shapes represented by the TF1G2D models. The high energy requirements for the dee shape had eliminated it from further consideration. The practical design difficulties of the inclined spring support for the tear-drop shape with T1 = T2 (see Figure 6), and the large tension jump which exists in the tear-drop shape with T1 $\neq$ T2 have also eliminated it from consideration. Manufacturing simplicity of the circular coil and its low-energy requirements were the important points for the selection of the circular configuration.

Figure 15 shows the casing stress versus location and stiffness of the double ring supports for the circular coil. This was obtained by using the TF2G2D model.

Using the TF1G3D model, a NASTRAN non-linear dynamic transient analysis was performed for the 0.42 Tesla Strong Compression plasma off run 41 EF load condition. This out-of-plane TF coil loading was applied to TF coil nodes as concentrated time dependent nodal forces. The load-time profile used is shown in the normalized strong compression EF current of Figure 16. Both dynamic and static analyses were made using the TF1G3D model. Comparisons of

the stresses obtained from the dynamic and static analyses were made to determine the dynamic effect of the operational EF loading. Typical stress multiplication factors for various parts of the TF coil structure were less than 1.09 except in the area near the pedestal support. The factor is 1.18 at the pedestal support. The tangential load transmitted to the floor at the pedestal increases from 0 (static loads) to 60 kips (dynamic load). This is due to the inertia load induced by the restraint at the pedestal. Similar results were obtained for the faulted load (one or more coil short-circuited) and seismic analyses. Both the faulted and seismic loads have little effect on the coil, whereas the pedestal receives a significant amount of loads.

A plot of maximum shear stress in the epoxy due to the TF and thermal loads from the TF3G2D model is shown in Figure 17. Since the model is 2-D, epoxy shear stress due to EF load is not available; it can be obtained from the 3-D model TF2G3D (see Figure 18).

The design criteria used for the coil case is basically derived from the ASME Boiler and Pressure Vessel Code. This code uses stress intensity, which is defined as the largest algebraic difference between any two of the three principal stresses. In order to facilitate the evaluation of coil case stress, all NASTRAN output for the TF2G3D model were post-processed and presented in both tabulated and plotted formats. A typical plot of membrane stress intensity is shown in Figure 19. A plot shown in Figure 20 was used by the designer in the determination of bolt requirement (the bolts fasten the coil side plate to the flange).

Stress distributions in various parts of the TF3G3D local model are shown in Figure 21. These results are for the early TF coil, with titanium as casing material. This model was not re-run for the latest configuration, since at that time the composite element was available for model development. However, the results from the early coil configuration served as a benchmark for the TF2G3D model.

The yoke load distribution calculated by using the yoke model is shown in Figure 22.

The major principal stress and the maximum stress intensity (twice of maximum shear) are presented in Table II. In general, the maximum principal stress is the tensile stress in the tangential direction of the TF coil. The stress level was mostly due to the by-passing stress; the radial pin load contributed about 15% to 18% and the tangential pin load contributed about 7%. The difference between the principal stress and the stress intensity was primarily due to the bearing (compressive) stress of the pin loads. In load cases 2 and 3, there were minor or no differences between the maximum principal stress and stress intensity, since no radial pin loads were directly applied at the edge of the bolt holes.

The stress levels in the coil components from the Composite Element model and the second generation 3-D model are compared in Table III. Despite the number of different model techniques used in these models, the stress levels were fairly close.

CONCLUDING REMARKS

There were sufficient NASTRAN diagnostics used in all models described in this paper such that good numerical results were obtained. Force balance at the inner support structure and selected coil nodal force balances were performed so that the confidence in these models was ascertained. Furthermore, the stress outputs from these models were compared and were found to be relatively close. The analysis results from these finite element models and the NASTRAN System were considered accurate enough to provide timely design information.

The application of available NASTRAN elements to the Tokamak toroidal field coil finite element models was considered very effective and the analysis results were acceptable. However, care should be taken in using the spring and isoparametric elements. Some of the comments pertaining to these elements are listed below:

- The plate element has no inplane rotational stiffness. Special care should be taken when it is connected to one-dimensional elements.
- The spring element used for non-colinear connection will induce unbalance moment.
- The nodal force balance output does not include the "lock-in" force induced by the thermal load.
- In a coarse model, the corner stresses for solid elements HEX8 and HEXA are not reliable.

The effect of the local detail design, such as the bolt joint connection between the sideplate and the flange, was neglected in the TF2G3D and other simplified models described in this paper. This effect will be analyzed separately when design detail is available.

REFERENCES

1. Chen, S.J., Heifetz, J., "The Toroidal Field Coil Stress Analysis - As Planned and Executed for the TFTR," Seventh Symposium on Engineering Problems of Fusion Research, Knoxville, Tennessee, October 1977.

2. Chang, H., Huang, N.S., "A 3-D Solid Finite Element for Heterogeneous Materials," Seventh Symposium on Engineering Problems of Fusion Research, Knoxville, Tennessee, October 1977.

Table I Finite Element Models

MODEL	OBJECTIVES	MODEL DESCRIPTION	LOADS
TF1G2D	• COIL SHAPE SELECTION • COIL SUPPORT SCHEME	• BAR, ELAS2 ELEMENTS • ONE-HALF OF COIL WITH SYMMETRIC BOUNDARY CONDITION	TF
TF2G2D	• COIL SUPPORT SCHEME • EFFECT OF INSULATION	• BAR, QDMEM2, ROD, SHEAR, ELAS2 ELEMENTS • ONE-HALF OF COIL WITH SYMMETRIC BOUNDARY CONDITION	TF
TF1G3D	• COIL SUPPORT SCHEME • DYNAMIC, SEISMIC, FAULT LOADS ANALYSES	• BAR, QUAD2, (QUAD4, ROD, ELAS2) ELEMENTS • TWO COILS WITH ROTATIONAL SYMMETRIC BOUNDARY CONDITION OR CYCLIC SYMMETRIC FEATURE	TF, EF, DYNAMIC, SEISMIC, FAULT
TF2G3D	• LOAD AND STRESS IN CASING • UPDATE DESIGNS • PROVIDE BOUNDARY COND FOR LOCAL MODELS • ESTIMATE STRESS INSIDE COIL	• QUAD2, HEX8, TRIA2, ELAS2 ELEMENTS • ONE COIL WITH ROTATIONAL SYMMETRIC BOUNDARY CONDITION OR CYCLIC SYMMETRIC FEATURE	TF, EF, THERMAL, DEAD
TF3G2D	• STRESS IN THE COPPER AND EPOXY • UPDATE DESIGNS	• BAR, SHEAR, ROD, QDMEM2 ELEMENTS • ONE-HALF OF COIL WITH SYMMETRIC BOUNDARY CONDITION • INCLUDE TWENTY-TWO LAYERS OF COPPER AND EPOXY INSULATION	TF, THERMAL
TF3G3D	• DETAILED STRESS IN THE CASING, COPPER, AND INSULATION AT THE CRITICAL NOSE AREA	• QUAD4, HEXA, WEDGE, SHEAR, ROD, BAR ELEMENTS • ONE-HALF OF 54.7° SEGMENT WITH SYMMETRIC AND ANTI-SYMMETRIC BOUNDARY CONDITIONS AND BOUNDARY FORCE FROM TF2G3D MODEL	TF, EF, THERMAL
90° YOKE SEGMENT	• BOLT LOADS AT THE OUTBOARD SUPPORT (YOKE)	• QUAD4, TRIA3, HEXA, ELAS2 ELEMENTS • 90° SEGMENT WITH THE BOUNDARY FORCE FROM TF2G3D MODEL	TF, EF, THERMAL
LOCAL STRESS CONCENTRATION	• PEAK STRESS AT THE BOLT HOLE OF SIDE WALL	• QUAD4, TRMEN ELEMENTS • APPROX 30° SEGMENT OF SIDE WALL WITH BOLT HOLES MODELED • MULTIPLE LEVEL SUPERELEMENT APPROACH USED	TF, EF, THERMAL
EBASCO COMPOSITE ELEMENT	• CONFIRMS PREVIOUS MODEL RESULTS • VERIFICATION OF COIL STRUCTURAL INTEGRITY	• EBASCO DEVELOPED COMPOSITE, SPRING AND PLATE ELEMENTS	TF, EF, THERMAL

Table II Peak Stress Near Bolt Hole

STRESS IN MPa (KSI)

CONFIG / STRESS / LOAD	8 IN. OUTER FLANGE		5¾ IN. OUTER FLANGE	
	MAXIMUM PRINCIPAL STRESS	MAXIMUM STRESS INTENSITY	MAXIMUM PRINCIPAL STRESS	MAXIMUM STRESS INTENSITY
LOAD CASE 1 (PIN LOAD IN TWO DIRECTION)	1036.3 (150.3)	1170.0 (169.7)	706.0 (102.4)	917.0 (133.0)
LOAD CASE 2 (PIN LOAD IN TANG DIRECTION)	872.2 (126.5)	872.2 (126.5)	578.5 (83.9)	637.1 (92.4)
LOAD CASE 3 (NO PIN LOAD)	807.4 (117.1)	807.4 (117.1)	526.8 (76.4)	526.8 (76.4)

NOTE: BOUNDARY FORCES WERE DERIVED FOR 3-D (TF2G3D MODEL) RUNS 2C26 AND 2C33B FOR TF + EF + THERMAL LOAD.

Table III TFTR Coil Comparison of Maximum Stresses (Toroidal Field, Equilibrium Field and Thermal Loads)

STRESS IN MPa (KSI)

MODEL NAME		COMPOSITE ELEMENT MODEL RUN CA-12A-2	TF2G3D MODEL RUN 2C33B
MODEL CHARACTERISTICS		1) ALL SOLID COMPOSITE ELEMENTS 2) COIL CONFIGURATION 12A 3) FINE GRID MODEL 4) 4-RING SOLID ELEMENT SUPPORTS 5) UNBONDED CASING AND CORE (NON-LINEAR SPRING)	1) PLATE ELEMENT FOR CASING, SOLID ELEMENTS FOR CORE 2) COIL CONFIGURATION 12A 3) FINE GRID MODEL 4) 4-RING PLATE ELEMENT SUPPORTS 5) UNBONDED CASING AND CORE (LINEAR SPRING WITH ITERATION)
CASING STRESS INTENSITY (MEMBRANE & BENDING)	INNER	252.3 (36.6)	250.3 (36.3)
	OUTER	292.3 (42.4)	289.6 (42.0)
	SIDE	283.4 (41.1)	262.7 (38.1)
COPPER HOOP STRESS		-137.9 (-20.0)	-101.4 (-14.7)
EPOXY SHEAR STRESS (R_ϕ)		20.0 (2.9)	23.4 (3.4) FROM TF2G3D AND TF3G2D

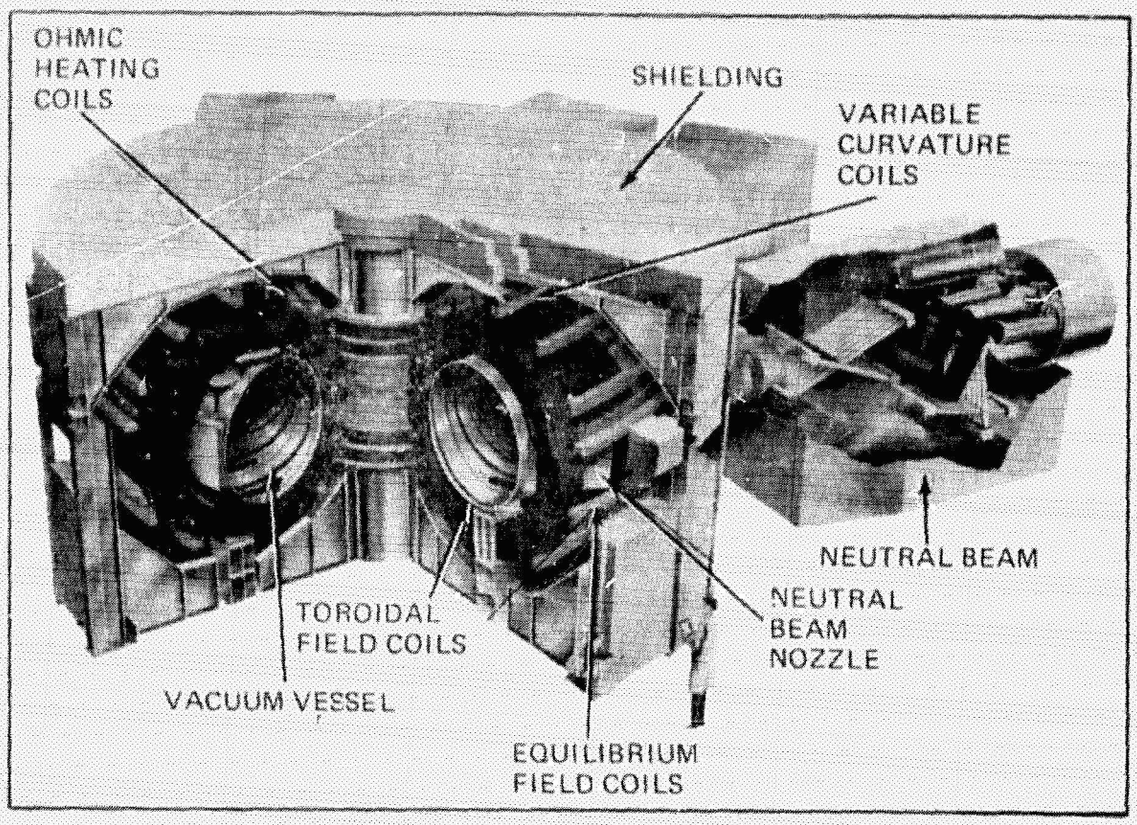

Figure 1 Tokamak Fusion Test Reactor

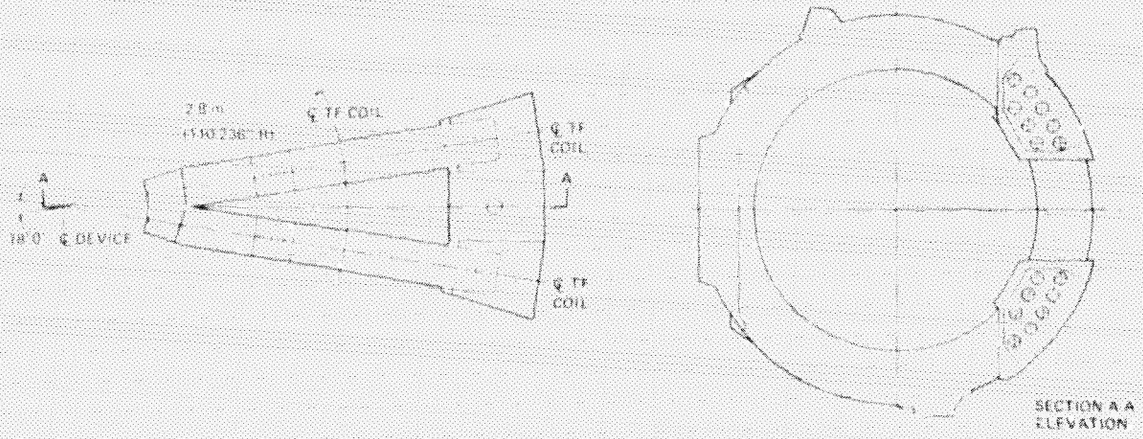

Figure 2 TF Coil Sector Assembly

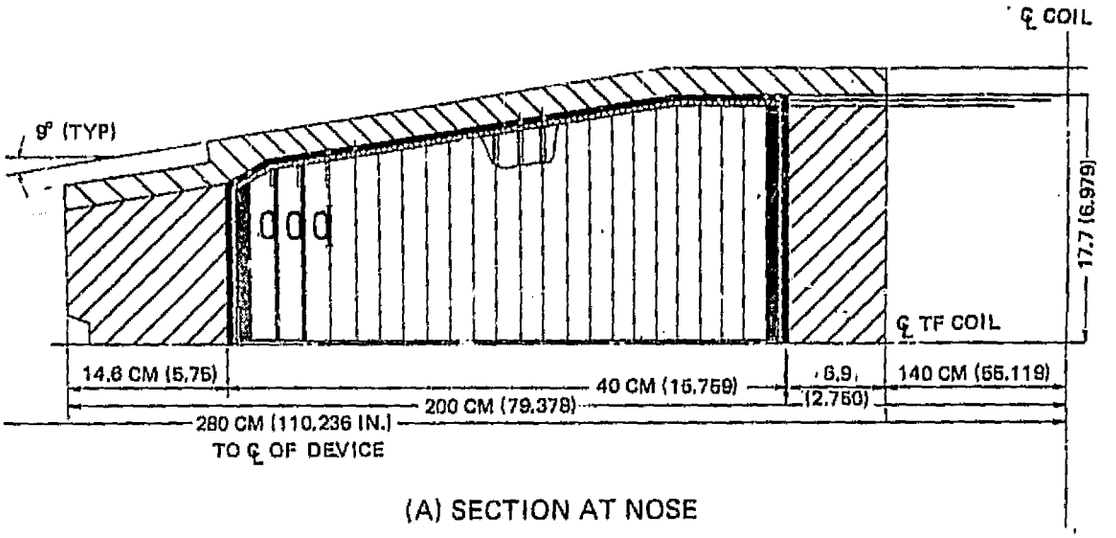

(A) SECTION AT NOSE

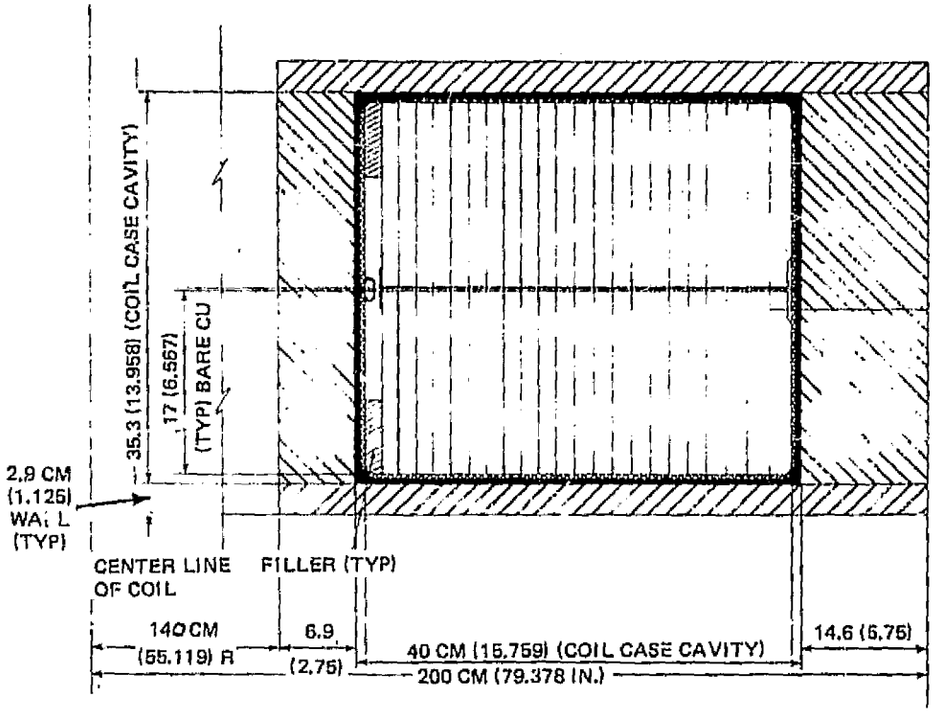

(B) TYPICAL SECTION

Figure 3 Typical Section of Coil Configuration

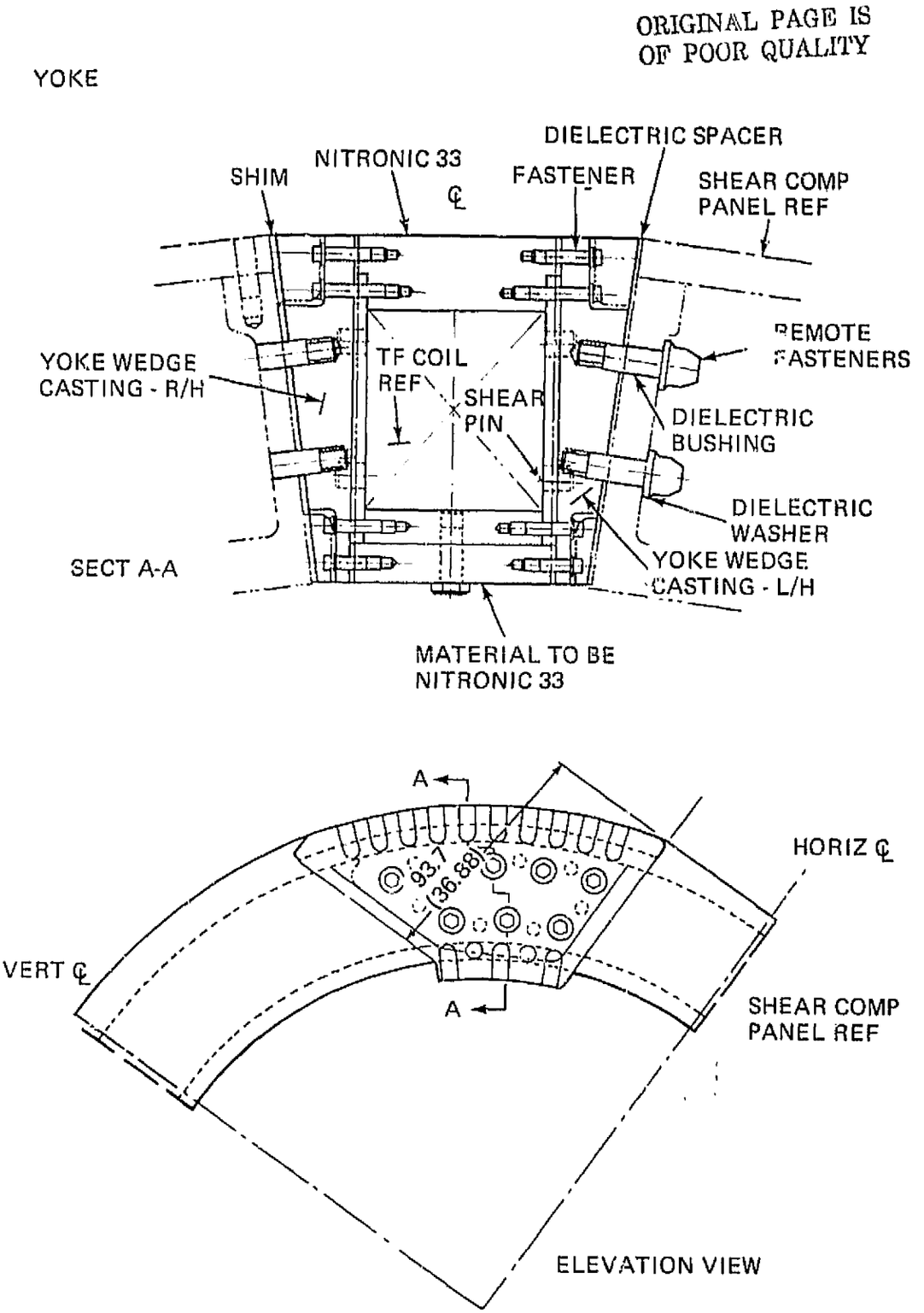

Figure 4 Shear-Compression Box and Yoke

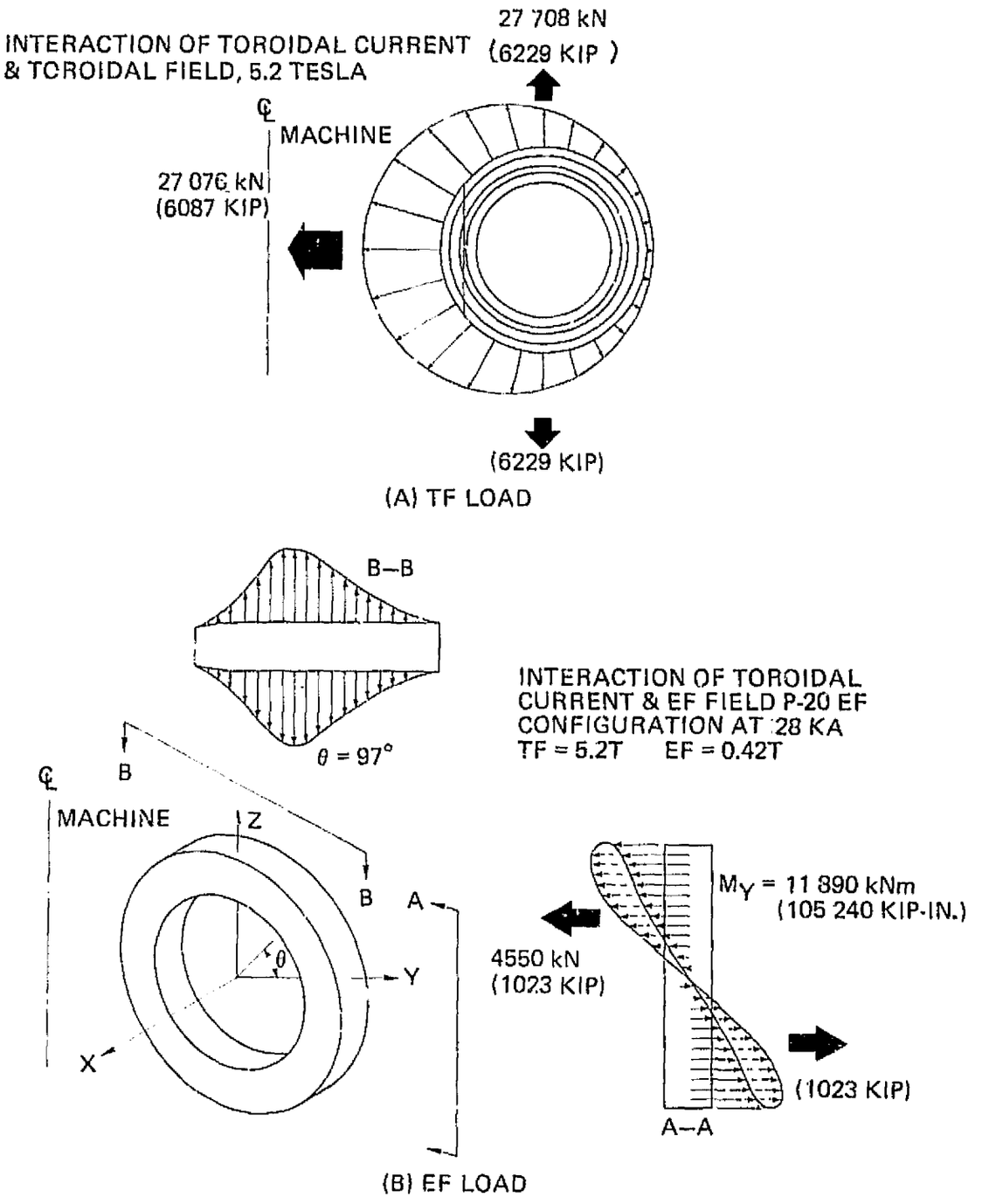

Figure 5 TF and EF Loads

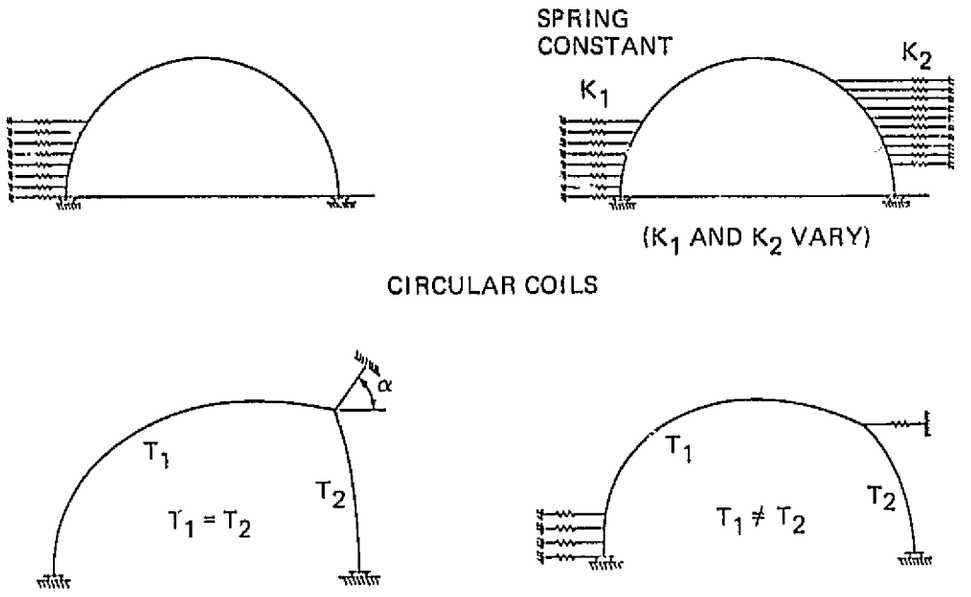

Figure 6 Configuration and Support of Coils (TF1G2D)

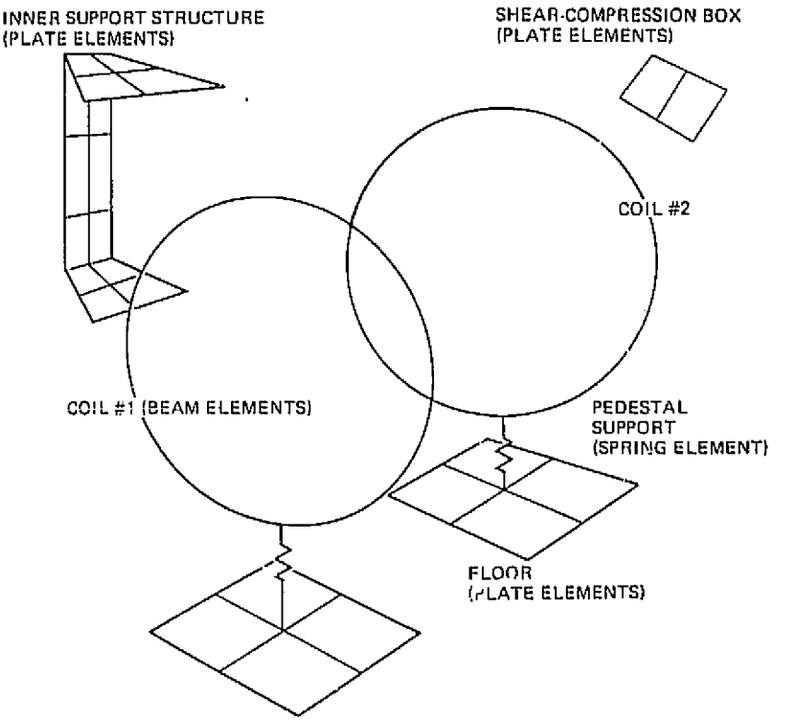

Figure 7 First Generation 3-D Model (TF1G3D)

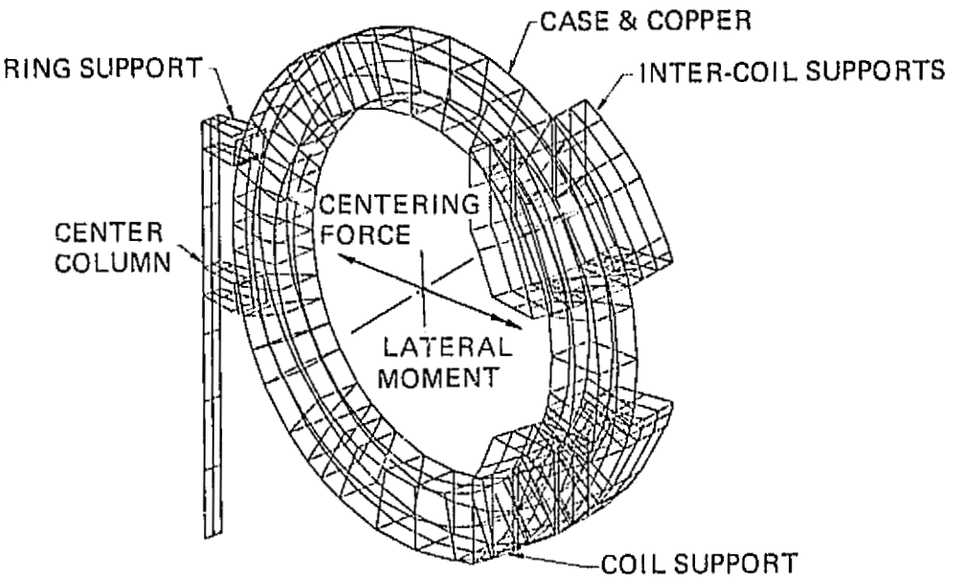

(A) TF COIL 3-D FINITE ELEMENT MODEL

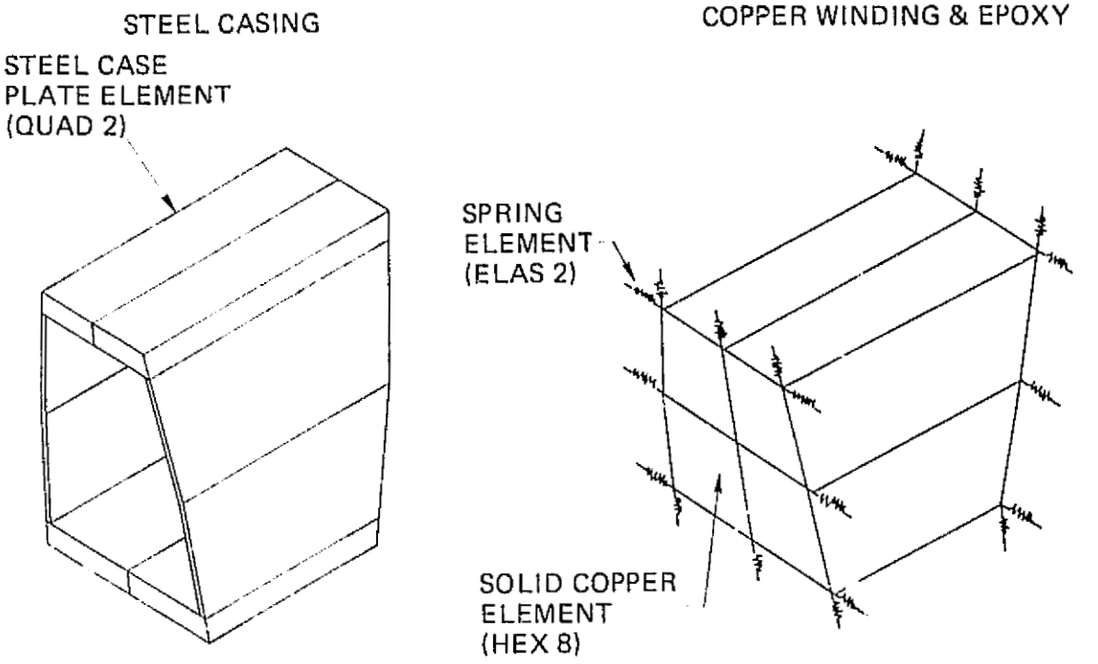

(B) COIL SEGMENT OF 3-D MODEL

Figure 8 Second Generation 3-D Model (TF2G3D)

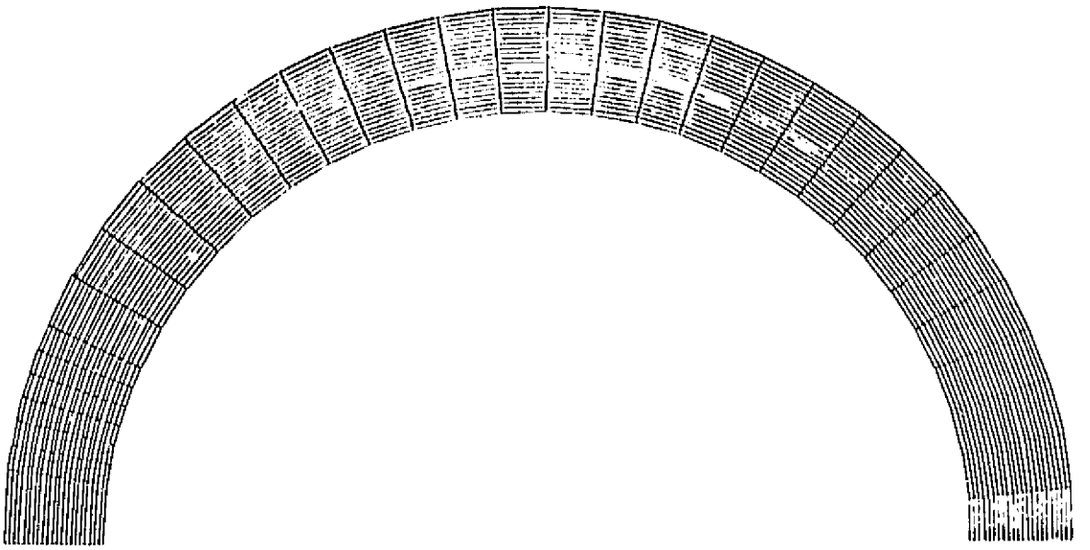

(A) SHEAR ELEMENTS

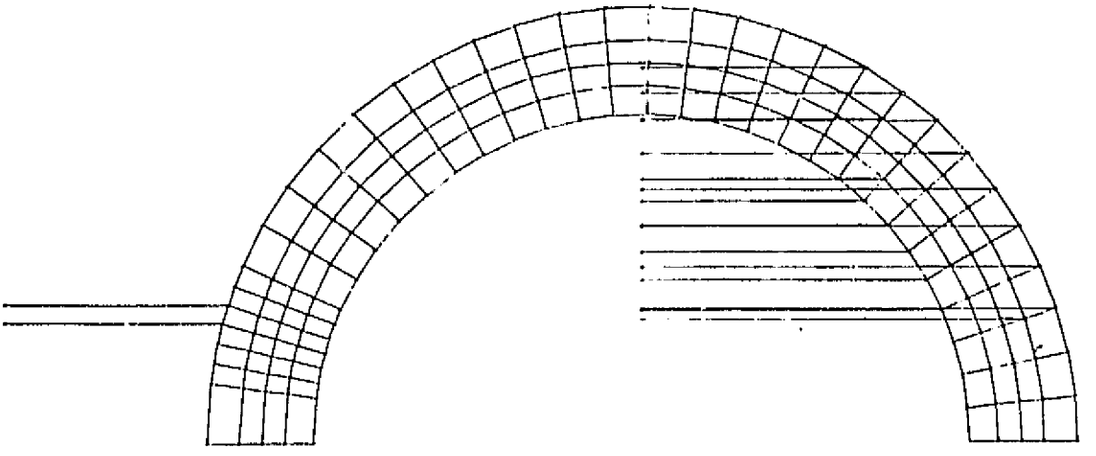

(B) QDMEM2 AND CONROD ELEMENTS AT SUPPORTS

Figure 9 Third Generation 2-D Model (TF3G2D)

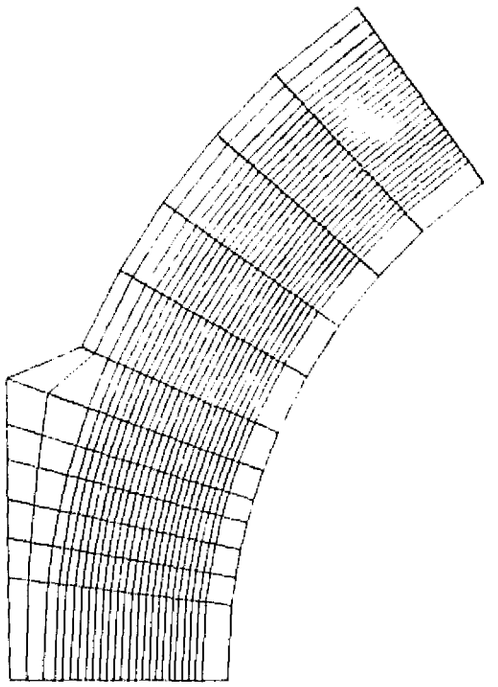

Figure 10 TF Coil 3-D Local FEA Model (TF3G3D)

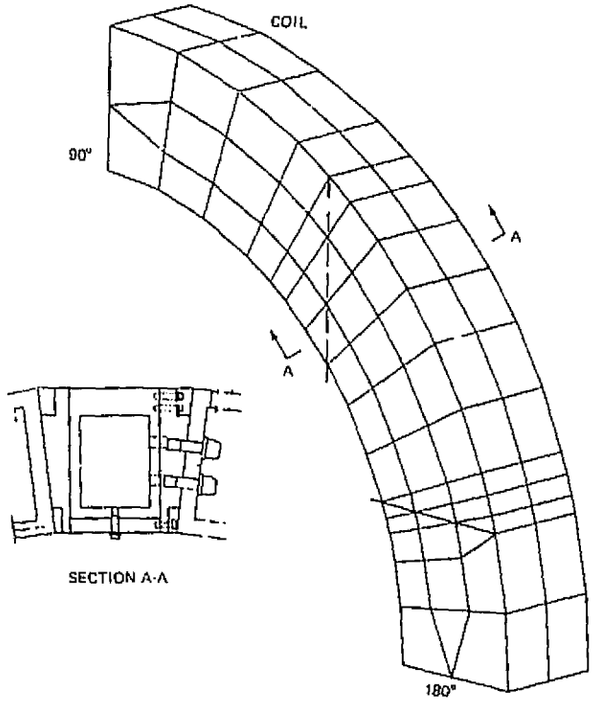

Figure 11 90^{o} Yoke Segment Model

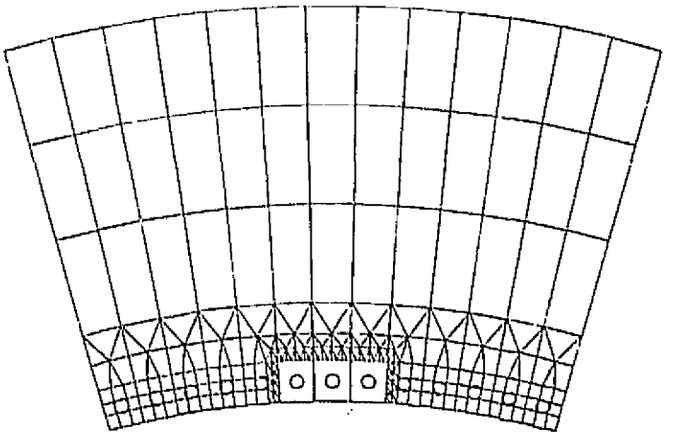

Figure 12 Residual Superelement

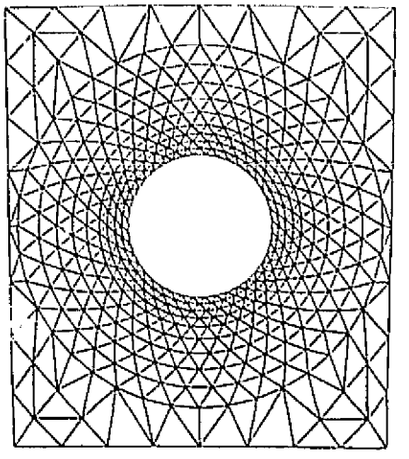

Figure 13 Primary Superelement

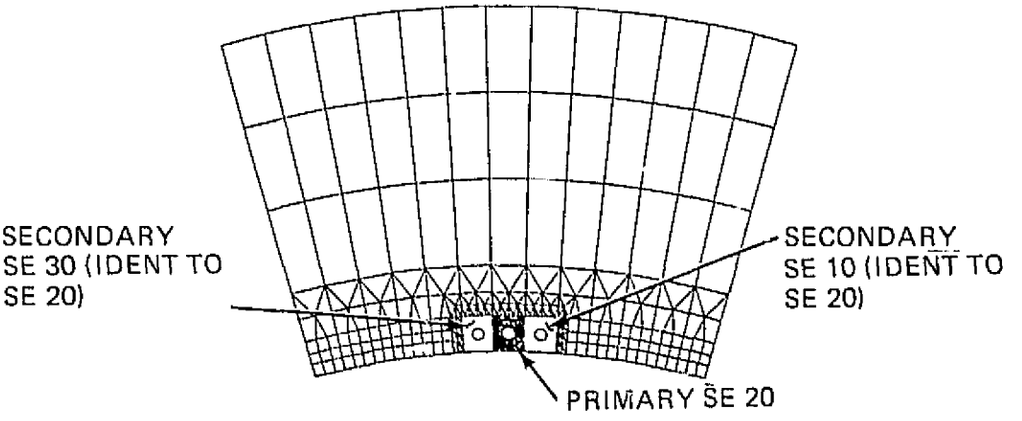

Figure 14 Remainder of Structure Considered SE 0 or Residual Structure

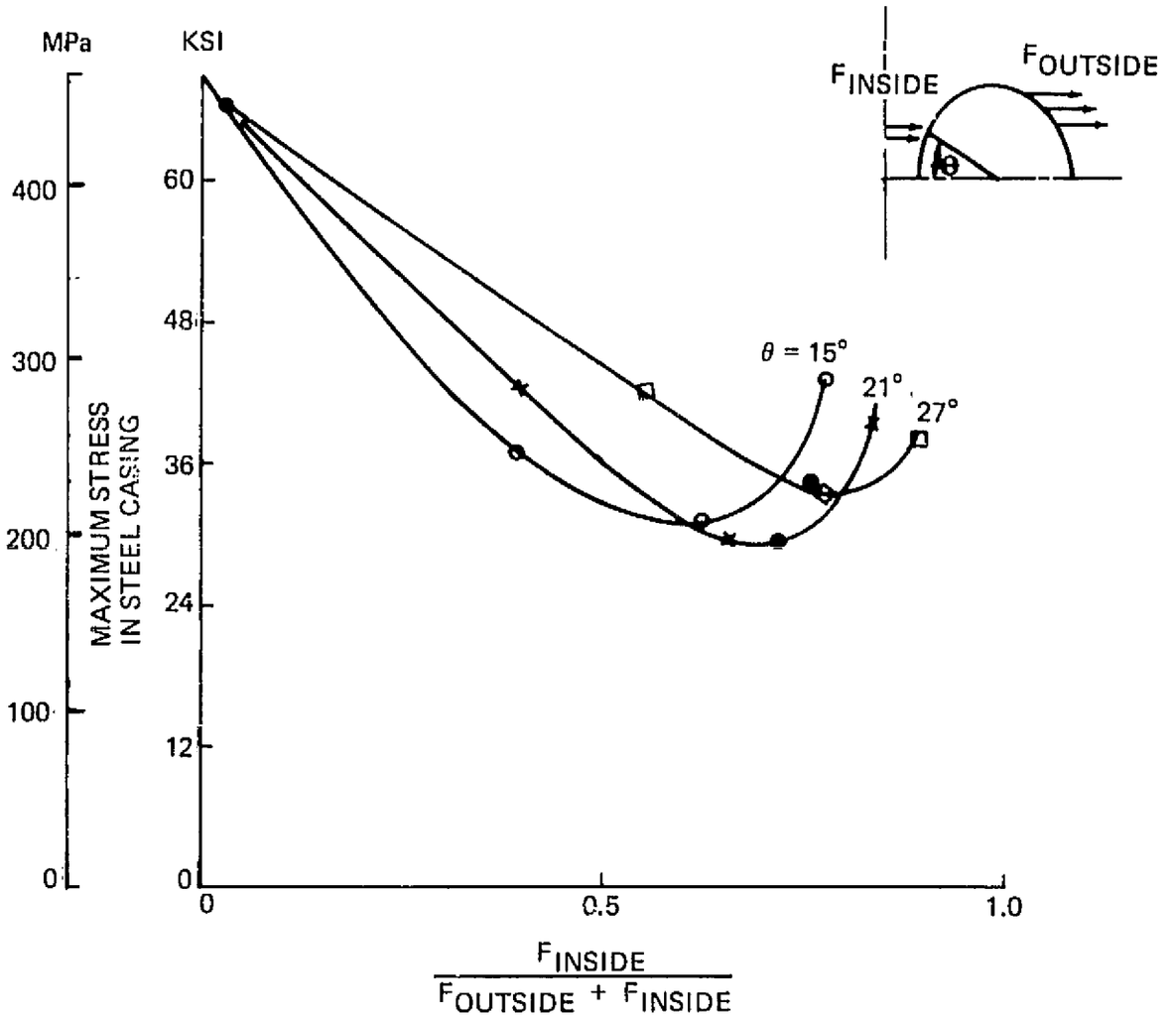

Figure 15 Maximum Stress in Steel Casing vs Stiffness and Location of Support (Represented by Force Ratio)

(A) TOROIDAL FIELD COIL FORCE – TIME SCENARIO FOR INPLANE LOADS

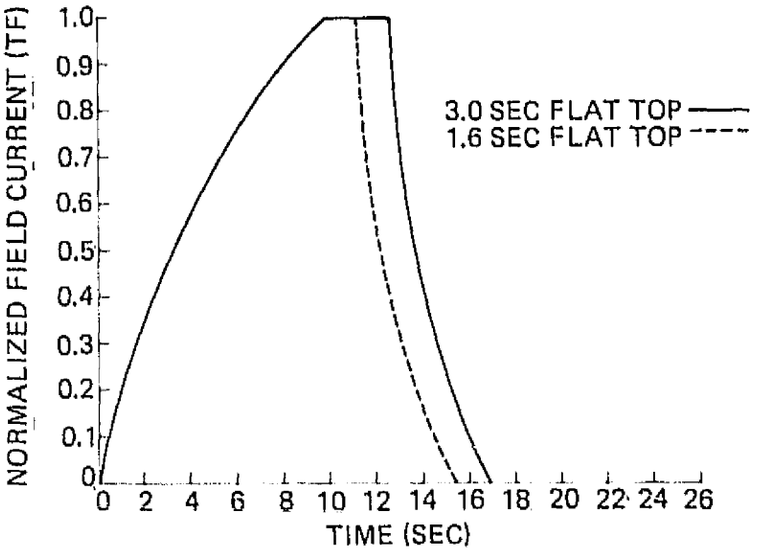

(B) TOROIDAL FIELD COIL FORCE – TIME SCENARIO FOR OUT-OF-PLANE LOADS

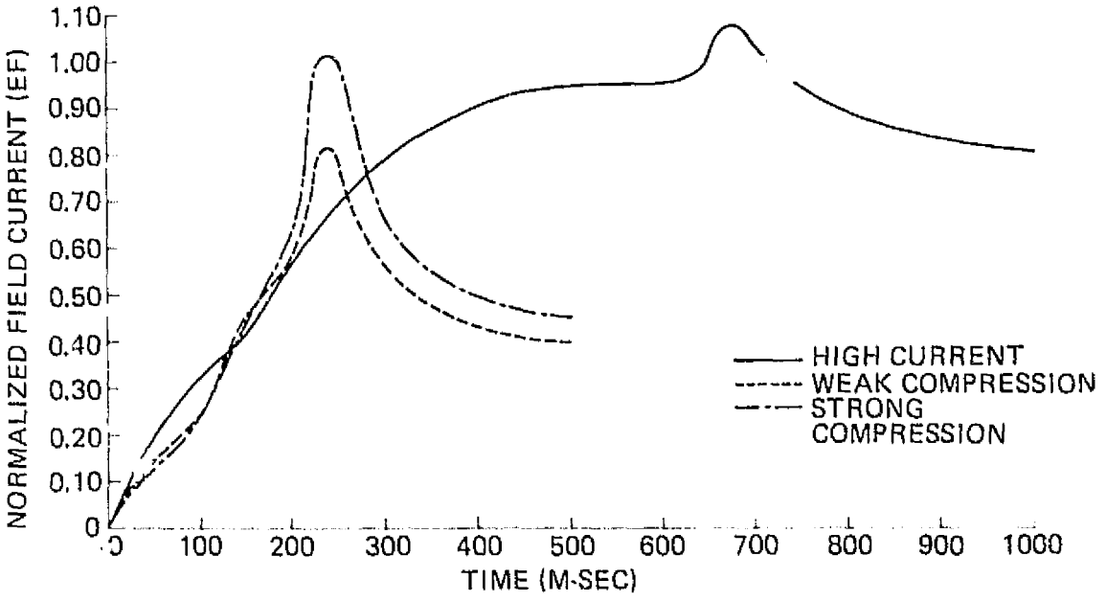

Figure 16 TF and EF Scenarios

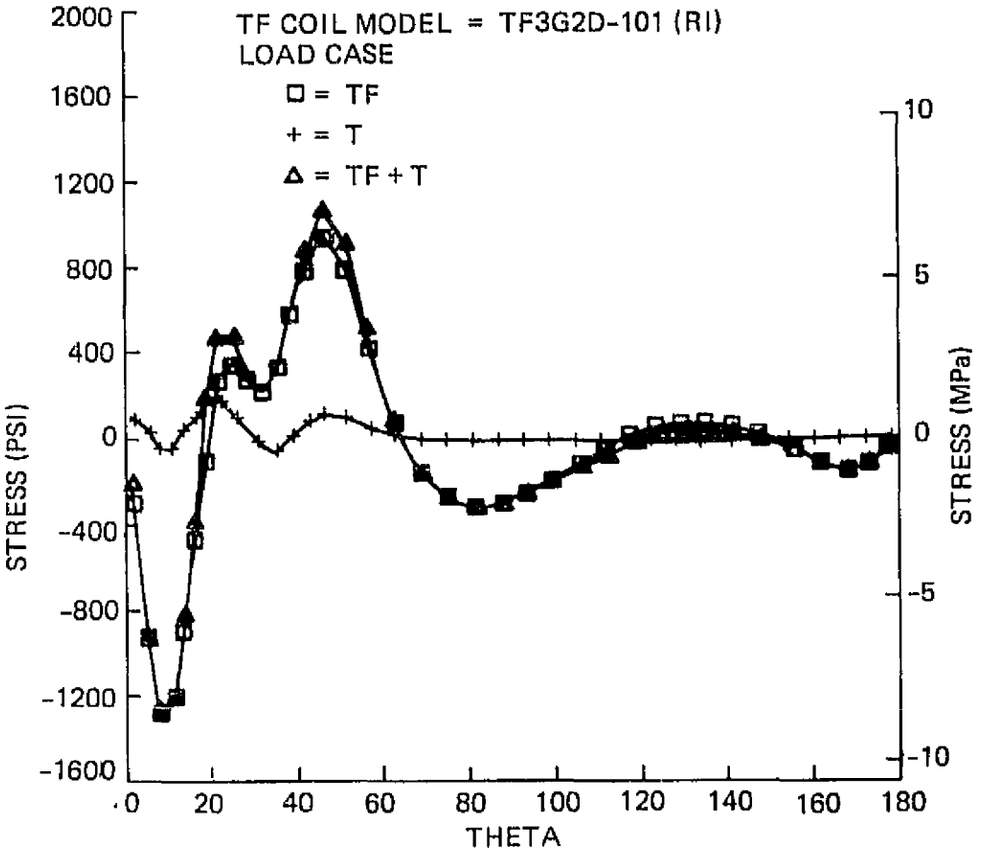

Figure 17 Epoxy Max Shear Stress

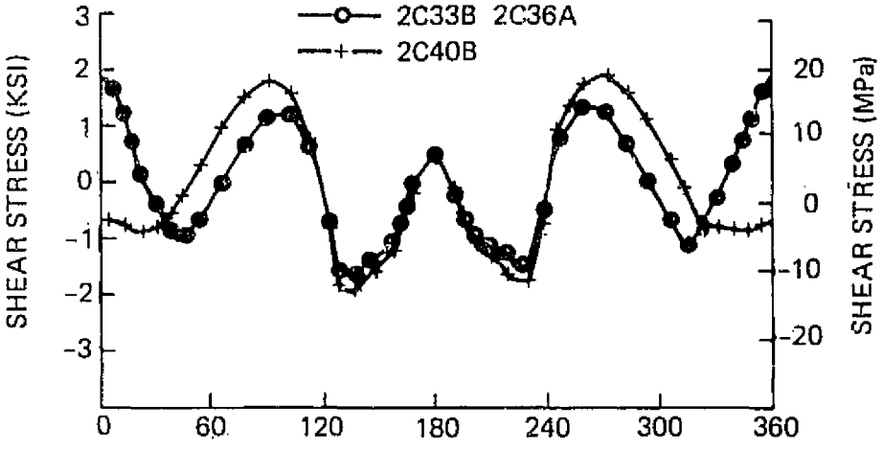

Figure 18 Estimated Shear Stress of Epoxy Due to Torque Induced by EF Load

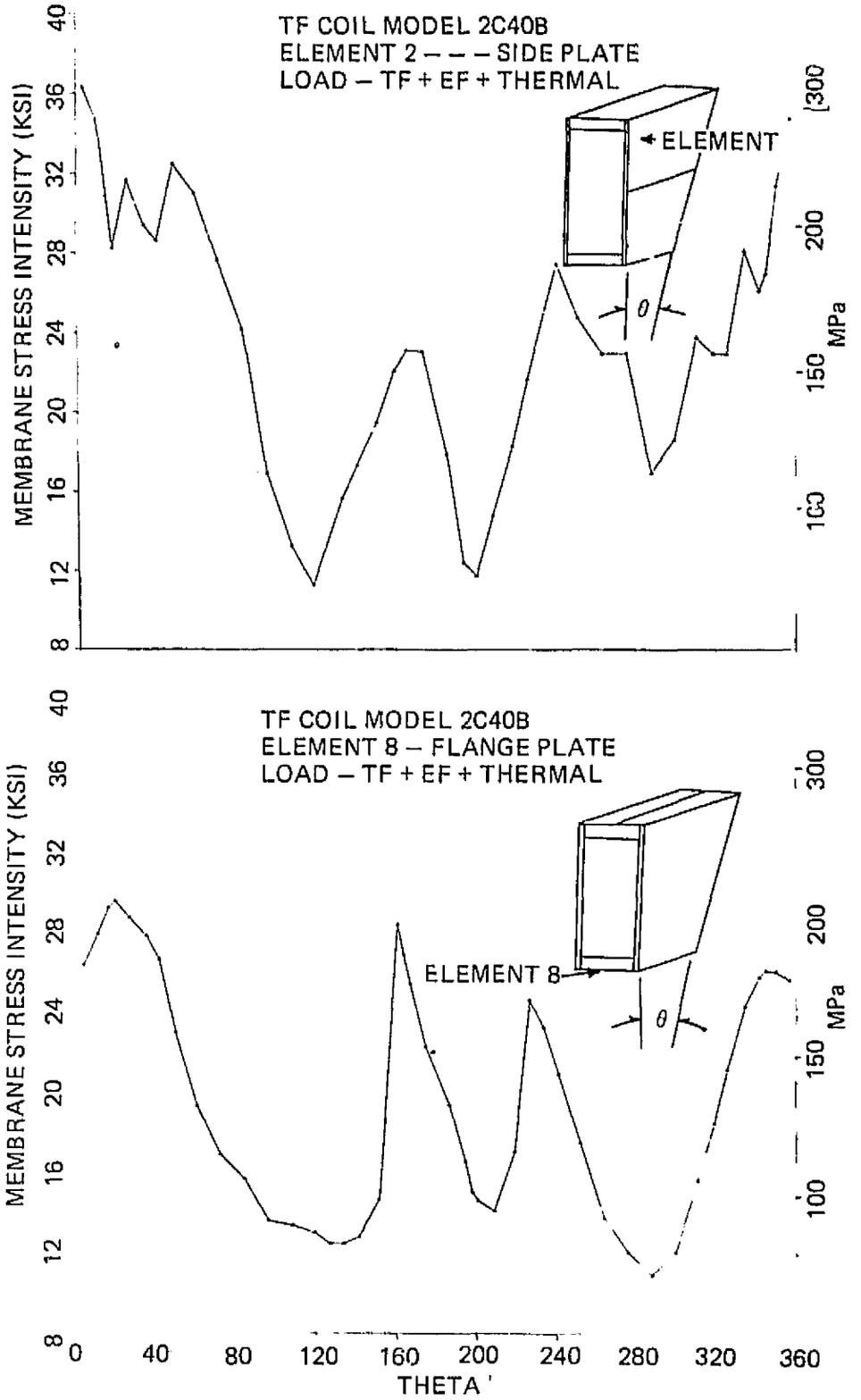

Figure 19 Typcial Membrane Stress Intensity

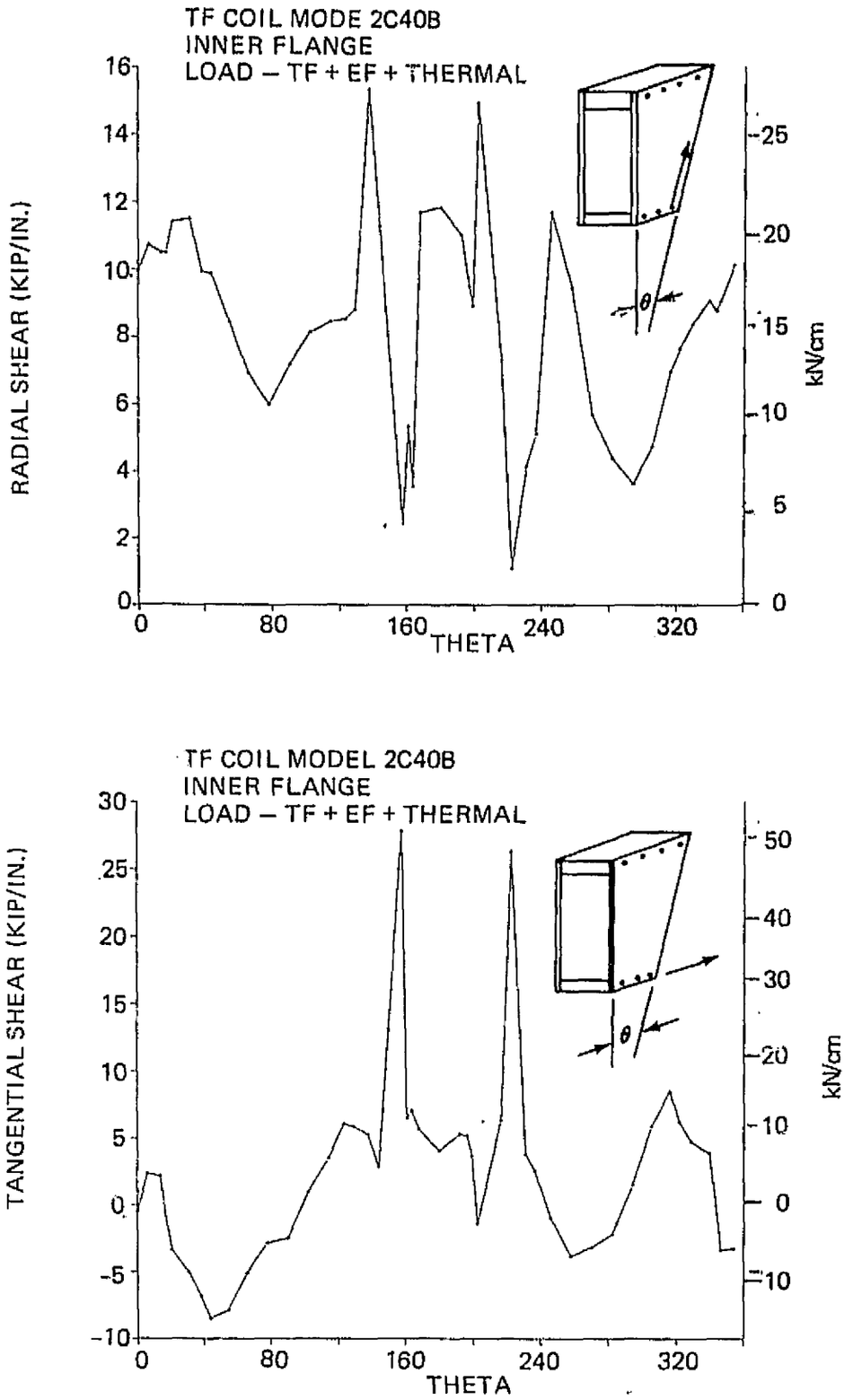

Figure 20 Typical Radial and Tangential Shear

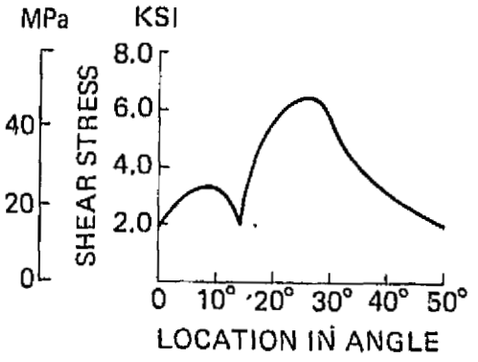

(A) MAXIMUM INTERLAMINAR SHEAR STRESS

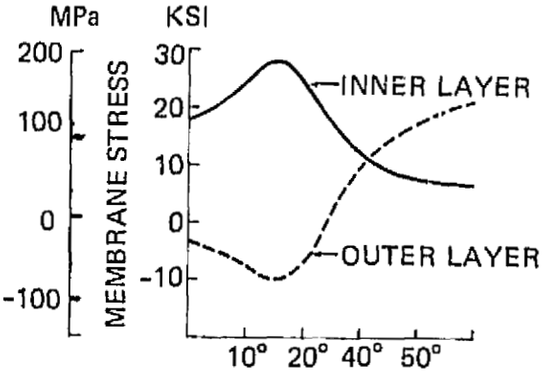

(B) COPPER STRESS IN HOOP DIRECTION

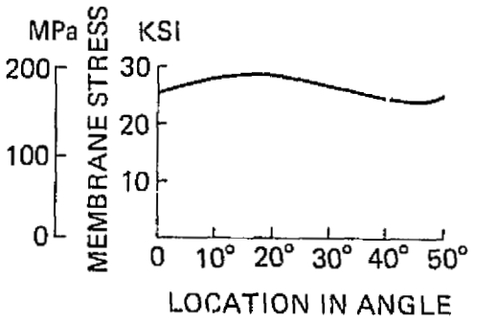

(C) INNER FLANGE STRESS IN HOOP DIRECTION

Figure 21 Stress Plots from Third Generation 3-D Local Model

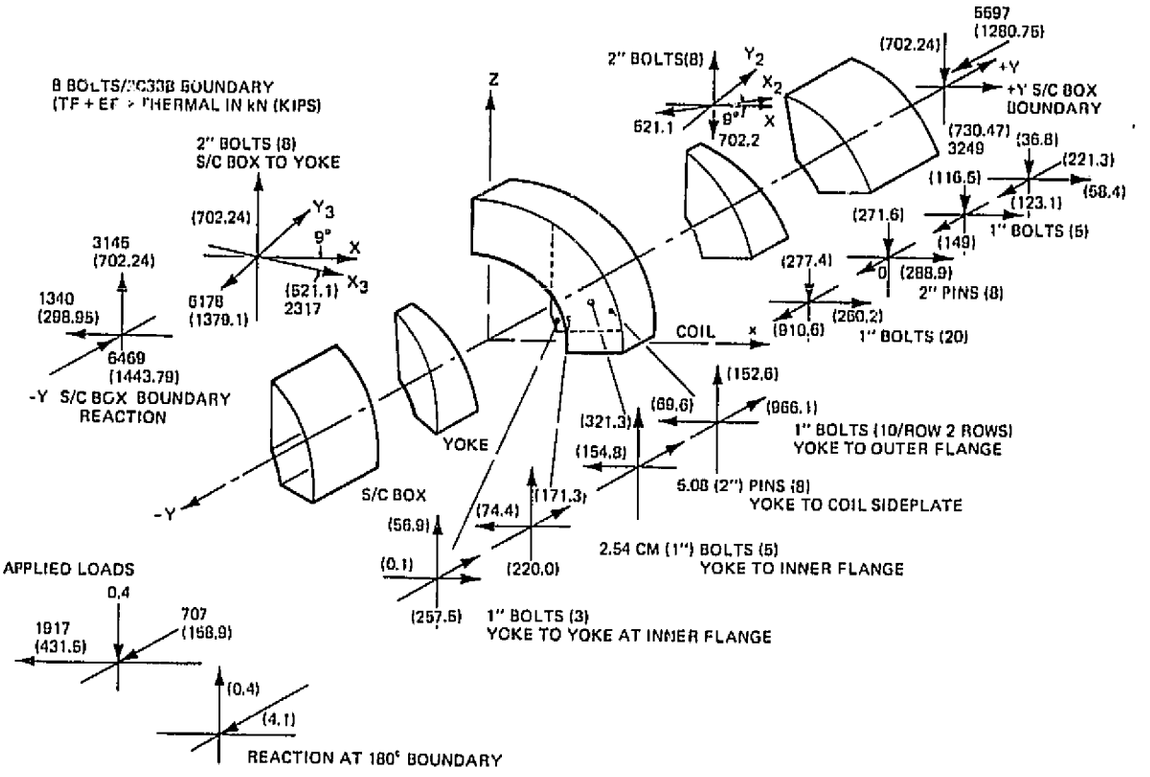

ORIGINAL PAGE IS
OF POOR QUALITY

Figure 22 Load Distribution Yoke Finite Element Model